A systematic coarse-scale model reduction technique for parameter-dependent flows in highly heterogeneous media and its applications

Yalchin Efendiev* Juan Galvis† Florian Thomines‡

May 10, 2012

Abstract

In this paper, we propose a multiscale approach for solving the parameter-dependent elliptic equation with highly heterogeneous coefficients. In particular, we assume that the coefficients have both small scales and high contrast (where the high contrast refers to the large variations in the coefficients). The main idea of our approach is to construct local basis functions that encode the local features present in the coefficient to approximate the solution of parameter-dependent flow equation. Constructing local basis functions involves (1) finding initial multiscale basis functions and (2) constructing local spectral problems for complementing the initial coarse space. We use the Reduced Basis (RB) approach to construct a reduced dimensional local approximation that allows quickly computing the local spectral problem. This is done following the RB concept by constructing a low dimensional approximation offline. For any online parameter value, we use a reduced dimensional approximation of the local problem to construct multiscale basis functions. These local computations are fast and are used to solve the coarse-scale dimensional problem. We present the details of the algorithm and numerical results. The locally supported basis functions can be used to obtain a coarse multiscale approximation for any smooth right hand side (source term). The approximation of the solution is obtained by solving a coarse global problem. The coarse problem can also be used to construct robust iterative methods of the domain decomposition type. Our numerical results show that one can achieve a substantial dimension reduction when solving the local spectral problems. We discuss convergence of the method, the construction of initial multiscale basis functions and the computational cost of the proposed method.

1 Introduction

Multiscale problems occur in many applications that include flow through porous media, composite materials, and so on. In many of these applications, the media properties can vary highly at the microscale. For

*Department of Mathematics and ISC, Texas A & M University, College Station, TX 77843

†Department of Mathematics and ISC, Texas A & M University, College Station, TX 77843

‡Ecole des Ponts - ParisTech, Champs-sur-Marne, F-77455 Marne-la-Vallée cedex 2 and INRIA, MICMAC project, 78153 Le Chesnay Cedex, France.

example, in flow through fractured porous media, the conductivity within fractures can be several orders of magnitude higher than the conductivity within the matrix. Fracture regions, that are main conduits of the flow, can have complex heterogeneities. Note that in this case traditional scale separation assumptions no longer hold and therefore, classical homogenization and upscaling techniques cannot be straightforwardly applied. The variation in the conductivities in the fracture and matrix brings an additional small scale into the problem that one needs to take into account when designing efficient coarse-grid simulation techniques and iterative solvers.

Numerical discretization of flow problems in such heterogeneous media results to large ill-conditioned systems of linear equations. Several approaches are proposed to solve such systems. Some approaches involve the solution on a coarse grid (e.g., [23, 17, 24, 25, 31, 1, 4, 12, 9, 26, 36, 38]). In these approaches, coarse-grid properties such as upscaled conductivities or multiscale basis functions are constructed that represent the media or the solution on the coarse grid. For solving high-contrast problems on a fine grid, robust iterative methods that converge independent of the contrast and multiple scales are needed (e.g, [35, 29, 21, 5] and references therein). There are many works that discuss similarities between solvers and multiscale methods, (e.g., [38]) in the context of multi-phase flow). We note that multiscale and upscaling techniques are designed to solve global problems on a coarse grid for multiple source terms and right hand sides. This provides additional computational gain as the coarse-grid properties do not need to be re-computed.

In many applications, one deals with parameter-dependent heterogeneous problems. For example, in the presence of uncertainties, the media properties are often parametrized where the parameter represents realizations of the media properties. A typical example is the conductivity field described by a two-point correlation function that represents the correlation of the spatial field. Via Karhunen-Loeve expansion, one can expand the conductivity field and this expansion contains parameters that are random variables and spatial fields that represent the modes of the covariance matrix. Each value of the parameter gives a realization of the conductivity field. In many other more complex cases (e.g., channelized permeability fields), the conductivity can also be parametrized. In these parameter-dependent cases, it can be expensive to apply multiscale or upscaling methods realization-by-realization (i.e., to compute effective properties for each realization). Indeed, many multiscale and upscaling methods involve elaborate procedures to compute basis functions that can be used for multiple source terms and right hand sides. E.g., one may need to construct several basis functions per coarse element (see discussions below) and the coarse regions, that are often dictated by e.g., source terms, can be large. In this setup, it is important to construct smaller dimensional problems to compute basis functions online inexpensively. These computations will be based on some offline procedures. In this paper, we borrow the main idea from the Reduced Basis (RB) approach to achieve dimension reduction.

The Reduced Basis (RB) approach is proposed in [28, 33] and has been successfully applied to many parameter-dependent problems. The main idea of RB is to construct a reduced model based on offline computations. The offline computation involves the solution of global problems that are used to compute new basis functions. The reduced models are used for online computations for each parameter, i.e., the problem is rapidly solved online for each parameter. In many cases, when the solution is smooth with respect to the parameter one can achieve a substantial dimension reduction and represent the solution space with a small dimensional space. RB relies on affine representation of the coefficients with respect to the parameter or functionals of the parameter to pre-compute bilinear forms that speed-up the computations. Affine representation assumption can be relaxed as noted in previous findings, e.g., [6]. Our goal is to use RB ideas in constructing multiscale basis functions and to speed-up the simulations.

In this paper, we use multiscale methods for high-contrast media developed in [16, 19, 20] for a single

parameter case. In these approaches, based on local spectral problems for each coarse region, we construct multiscale basis functions to approximate the solution. The construction of coarse spaces starts with an initial choice of multiscale basis functions that are supported in coarse regions sharing a common node. The initial multiscale basis function is chosen to represent important features of local solutions for all parameter values. These basis functions are complemented using weighted local (parameter-dependent) spectral problems that are defined in coarse blocks sharing a common node. The weight function in the local spectral problem is computed based on the initial choice of multiscale basis functions. Furthermore, we identify important eigenvalues (small eigenvalues in our case, see discussion below) and corresponding eigenvectors that represent important features of the solution. Coarse spaces are constructed by multiplying the selected eigenvectors with the initial multiscale basis functions. These eigenvectors represent features that can not be localized with initial multiscale space.

For parameter-dependent problems, solving the local eigenvalue problem for each parameter at the online stage can be expensive, especially for the cases of large-size coarse blocks. RB offers an excellent opportunity to reduce the local eigenvalue problem to a problem with much smaller dimension. In particular, first, at the offline stage, we identify important eigenvectors for a range of parameters. Then, we use the RB technique to formulate a small dimensional spectral problem and downscaling operator that allows for solving the local spectral problem inexpensively in the online computations stage. At the online stage, for any parameter, we can rapidly compute multiscale basis functions. These basis functions are computed by solving small dimensional eigenvalue problems and selecting important eigenvectors for basis function construction. These eigenvectors are downscaled using a pre-computed multiscale interpolation operator. Furthermore, the coarse space is constructed and the global problem is solved. The dimension of the coarse system is related to important local features of the solution and it is the same as in standard multiscale methods with local spectral basis functions. However, the cost of computing a basis function is much smaller.

The coarse spaces constructed in this paper are targeting two main goals:

- obtaining robust convergence results of coarse multiscale approximations;
- obtaining robust bounds for the condition number of iterative (two-level additive) methods to compute fine-scale finite element solutions.

We show numerically (see Section 4) that the estimate for the convergence of MsFEM and the condition number of two-level preconditioners depend on the maximum of the inverse of the eigenvalues whose eigenvectors are not included in the coarse space. The maximum is taken over all coarse nodes. In order to obtain an optimal dimensional coarse space, the initial multiscale spaces are important. See [16, 19, 20]. We discuss possible choices for initial multiscale spaces for the parameter-dependent problem in Section 3.1.

The proposed methods have advantages over standard multiscale methods when applied to parameter-dependent problems. Our new approaches use pre-computed solutions calculated for some values of parameters, that are identified with RB methods, to speed-up the computations. Moreover, these basis functions can be used independent of the source terms which can not be done for general smooth right hand sides when global snapshots are employed. For multiscale problems, applications of reduced basis approaches that employ global snapshots are computationally expensive and the number of basis functions that are needed for calculating the solution at the online stage can be large. The proposed methods alleviate these problems (see Section 4.3). In particular, one does not need all snapshots when computing the solution at the online stage. This is because many of these global snapshots can be eliminated at the coarse-grid level by choosing appropriate basis functions. Our proposed approach can be especially useful when the

parameter itself is a coarse-grid spatial function where the parameter in each coarse block is assumed to be an independent scalar quantity. In this case, one has a very large dimensional parameter space, and approaches such as the ones proposed in this paper are needed for efficient computations because local problems will involve only a scalar parameter. Finally, the applications to domain decomposition methods and solvers are new. In our methods, solvers are regarded as the correction to the coarse-grid solution at the online stage. We show that one can use the offline coarse spaces to obtain robust preconditioners.

The proposed approaches share similarities with approaches where the RB is used in homogenization or MsFEM setting to solve local problems (e.g., [7, 30]). In these approaches, via offline computations, one reduces the cost associated with computing local solutions. Unlike the proposed approaches, these approaches do not systematically add new degrees of freedom on a coarse-grid level and do not consider high-contrast multiscale problems. Moreover, using our proposed coarse spaces, we construct robust contrast-independent preconditioners for multiscale problems. The proposed methods also have some relation to ensemble level multiscale methods [10, 2]. In ensemble level approaches, several realizations of the conductivity field are chosen and based on these realizations, multiscale basis functions are constructed for the whole ensemble or a part of the ensemble. Thus, one can construct a small dimensional space to span the solution for each member of the ensemble. In the proposed approaches, we speed-up basis computations to reducing these problems to much smaller dimensional ones at the online stage.

We present some representative numerical results. In our examples, we consider parameter-dependent high-contrast permeability fields where various distinct permeability features appear for different values of the parameter. We show numerically (see Section 4) that using our proposed technique one can substantially reduce the computational cost without sacrificing the accuracy of the method. We consider both coarse-grid approximation and the condition number for the preconditioned system where coarse spaces are inexpensively computed for each online parameter based on reduced dimensional local systems. We discuss the choice of initial multiscale basis functions designed for the entire parameter range. We show numerically (see Section 4) that if one can incorporate small-scale features (smaller than the coarse region) associated with all parameters into initial basis functions , we can achieve a dimension reduction for the coarse spaces. We discuss convergence of the method based on numerical experiments and computational cost (see Sections 4.1 and 4.3). Our proposed approach has lower computational cost, in general, compared to standard RB approaches that use global solutions. The computational gain is due to the fact that at online stage, we do not need all features that are in global solutions when standard RB is used. Via local solutions and online basis computations, we can identify small dimensional coarse spaces that are needed to compute the solution online without sacrificing the accuracy. Moreover, local computations can be performed in parallel and thus the computational time of solving local problems will be equivalent to that of solving one local problem. Our numerical results show that the combination of RB and MsFEM can provide an efficient computational tool for solving large-scale parameter-dependent multiscale problems with the parameter possibly varying over the coarse regions.

The paper is organized in the following way. In the next section, we present some background discussion on multiscale spaces, the RB, and two-level preconditioners. In Section 3, the details of the proposed algorithm are discussed. Numerical results and further discussions are presented in Section 4.

2 Preliminaries

We consider the following parameter-dependent problem

$$-\text{div}(\kappa(x;\mu)\nabla u) = f \ \text{ in } D \tag{1}$$

subject to some boundary conditions, where

$$\kappa(x;\mu) := \sum_{q=1}^{Q} \Theta_q(\mu)\kappa_q(x). \tag{2}$$

Here, $\kappa_q(x)$ is the heterogeneous spatial field with multiple scales and high contrast (e.g., see Figure 6 for an example of such a permeability field), the parameter $\mu \in \Lambda \subset \mathbb{R}^p$ is possibly a coarse grid function and the functions $\Theta_q : \Lambda \to \mathbb{R}$. We define the weak formulation of the problem (1) as follow

$$a(u_0, v; \mu) = f(v), \quad \text{for all } v \in H_0^1(\mathcal{D}), \tag{3}$$

with

$$a(u, v; \mu) = \int_D \kappa(x;\mu)\nabla u(x)\nabla v(x)dx \quad \text{for all } u, v \in H_0^1(D) \tag{4}$$

and

$$f(v) = \int_D f(x)v(x)dx \quad \text{for all } v \in H_0^1(D).$$

Next, we introduce the notation for the coarse grid and briefly introduce the main concept of multiscale finite element methods. Let $\mathcal{T}^H$ be a usual conforming partition of D into finite elements (triangles, quadrilaterals and etc.). We call this partition the coarse grid and assume that the coarse grid is partitioned into fine-grid blocks. We denote by N_v the number of coarse nodes, by $\{y_i\}_{i=1}^{N_v}$ the vertices of the coarse mesh $\mathcal{T}^H$ and define the neighborhood of the node y_i by

$$\omega_i = \bigcup \{K_j \in \mathcal{T}^H; \quad y_i \in \overline{K}_j\} \tag{5}$$

(see Figure 1) and the neighborhood of the coarse element K by

$$\omega_K = \bigcup \{\omega_j \in \mathcal{T}^H; \quad y_j \in \overline{K}\}. \tag{6}$$

Our objective is to construct a coarse-grid reduced order model, so that for any value of the parameter μ and any value of the right hand side f we will be able to compute, in a very efficient way, the solution to (1).

To obtain numerical approximations of (1), we will compute *numerically* a set of multiscale basis functions for each node y_i. We denote the basis functions for the node i, $\chi_i^\ell (= \chi_i^\ell(x;\mu))$, and assume that the basis functions are supported in ω_i. As in standard finite element methods, once multiscale basis functions are constructed, we seek $u_0 = \sum_{i\ell} c_{i\ell}\chi_i^\ell$, where $c_{i\ell}$ are determined from a standard Galerkin projection

$$a(u_0, v; \mu) = f(v), \quad \text{for all } v \in V_0, \tag{7}$$

where $V_0 = \text{span}\{\chi_i^\ell\}$ that vanish on the boundary of D. Once $c_{i\ell}$'s are determined, one can define a fine-scale approximation of the solution by reconstructing via basis functions, $u_0 = \sum_{i\ell} c_{i\ell}\chi_i^\ell$.

As the multiscale basis function are *adapted* to the *specific* oscillation present in the coefficient, they strongly depend on μ. It is often expensive to compute multiscale basis functions as one may need to solve local spectral problems to find an appropriate number of basis functions. Moreover, for the MsFEM to be accurate, we need to define a new basis for each single value of the parameter μ. For this purpose we will construct a reduced order problem to compute the basis function. The construction of the basis involves

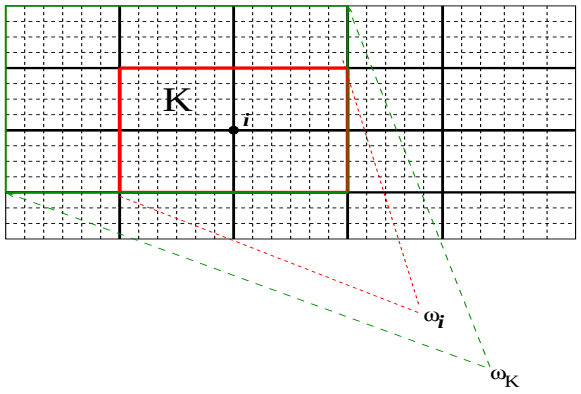

Figure 1: Schematic description of coarse regions.

the approximation of local parametric eigenvalue problems. We will be applying reduced basis techniques to these local parametric eigenvalue problems posed on coarse regions.

We will also use coarse spaces constructed via the RB technique in two-level additive Schwarz preconditioners (e.g., [29]). Our main goal is to show that with these basis functions one can obtain optimal (in terms of contrast) preconditioners. Next, we briefly describe the two-level domain decomposition setting that we use. We denote by $\{D_i'\}_{i=1}^M$ the overlapping decomposition obtained from the original non-overlapping decomposition $\{D_i\}_{i=1}^M$ by enlarging each subdomain D_i to

$$D_i' = D_i \cup \{x \in D, \text{dist}(x, D_i) < \delta_i\}, \quad i = 1, \ldots, M, \tag{8}$$

where dist is some distance function and let $V_0^i(D_i')$ be the set of finite element functions with support in D_i' and zero trace on the boundary $\partial D_i'$. We also denote by $R_i^T : V_0^i(D_i') \to V^h$ the extension by zero operator.

We consider iterative methods to find the solution of the fine-grid finite element problem

$$a(u, v; \mu) = f(v), \quad \text{for all } v \in V^h, \tag{9}$$

where V^h is the fine-grid finite element space of piecewise linear polynomials and the bilinear form a defined in (4). The matrix of this linear systems is written as

$$A(\mu)u(\mu) = b.$$

Here, A is the stiffness matrix associated to the bilinear form a and b is such that $v^T b = f(v)$ for all $v \in V^h$. We note that we are representing finite element functions and their vector of coordinates by the same symbols. We can solve the fine-scale linear system iteratively with the preconditioned conjugate gradient (PCG) method. Any other suitable iterative scheme can be used as well. We introduce the two level additive preconditioner of the form

$$B^{-1}(\mu) = R_0^T(\mu) A_0^{-1}(\mu) R_0(\mu) + \sum_{i=1}^{M} R_i^T A_i^{-1}(\mu) R_i, \tag{10}$$

where the local matrices are defined by

$$vA_i(\mu)w = a(v, w; \mu) \quad \text{for all } v, w \in V_0^i(D_i'). \tag{11}$$

The coarse projection matrix R_0^T is defined by $R_0^T = R_0^T(\mu) = [\Phi_1, \ldots, \Phi_{N_v}]$ and $A_0(\mu) = R_0(\mu)A(\mu)R_0^T(\mu)$. The columns Φ_i's are fine-grid coordinate vectors corresponding to the basis functions $\{\chi_i^j\}$. See [35, 29] and references therein. In this paper, we will use RB procedures to construct (approximations of) the coarse space basis, i.e., $R_0(\mu)$, for any given value of the parameter μ.

The application of the preconditioner involves solving local problems in each iteration. In domain decomposition methods, our main goal is to reduce the number of iterations in the iterative procedure. It is well known that a coarse solve needs to be added to the one level preconditioner in order to construct robust methods. The appropriate construction of the coarse space V_0 plays a key role in obtaining robust iterative domain decomposition methods.

In the numerical experiments, we will assume that the overlapping subdomains $\{D_i'\}$ coincide with the coarse vertex neighborhoods $\{\omega_i\}$ of $\mathcal{T}^H$. In this case $\delta \asymp H$, where $\delta = \max_{1\leq i\leq N} \delta_i$ is the overlapping parameter.

Next, we briefly describe basic concepts of the reduced basis approach that employs global snapshots to construct reduced-order models for computing the solution of the parameter-dependent elliptic problem. The RB method can be understood as a way to discretize the manifold $\mathcal{E} = \{u(x; \mu), \mu \in \Lambda\}$; otherwise stated it consists of defining a finite dimensional space $X_N = \text{Span}\{u(x; \mu_m), 1 \leq m \leq N\}$, where N is *small*. Once X_N has been defined, we compute the solution using a standard Galerkin projection:

$$a(u, v; \mu) = f(v), \quad \text{for all } v \in X_N, \tag{12}$$

with a defined in (4). The problem above is equivalent to solving a linear problem of dimension N and is thus cheap provided that N is small. We thus are left with the definition of the basis of X_N, which is done by computing N snapshots (i.e., solution of the original equation for a given value of the parameter μ_m). A Greedy algorithm (see Section 3.3 below) is used to select iteratively the snapshots. Note that in the methods proposed in this paper, RB is used locally to construct multiscale basis functions that can be used to solve the global problem on a coarse grid.

3 Coarse-scale model reduction. Reduced Basis Multiscale Finite Element Method (RB-MsFEM)

In this section, we describe how coarse spaces are constructed. The main idea of this construction is to start with an initial multiscale basis functions which capture the effects that can be localized within coarse regions, this step is described in Section 3.1. Furthermore, we introduce, in Section 3.2, a local spectral problem where initial multiscale space is used to construct the weight function for this spectral problem. The eigenvectors corresponding to small eigenvalues represent important features of the solution (in energy norm). These eigenvectors are multiplied by initial basis functions to form the coarse space.

In order to speed-up the computation of the spectral problems in a parameter dependent case, we use the RB techniques (see Section 3.3). Note that the computation of local eigenvalue problem for each coarse domain and for each online parameter can be expensive (see Section 4.3). We thus perform offline computation to pre-compute all the stiffness matrices needed for basis calculations and their reduced representation as well as the downscaling operators that allow us to easily go from the reduced basis to

the fine mesh basis. The online stage (see Section3.4) is a two step computation where first we solve on each coarse region, for a given value of μ, the reduced problems that yield the multiscale basis functions and then compute the solution of the initial problem for a given value of the right hand side f. First, we describe some essential ingredients needed for our method and in Section 3.5, we will summarize our algorithm.

3.1 Initial basis functions

First, we briefly discuss the construction of the initial basis functions as they are used in setting up local spectral problems (see Item 3 of the offline stage). As we mentioned, initial multiscale basis functions are chosen such to include the features of the solution for all parameters μ. For this reason, we need to identify a permeability that contains as many of the small-scale features as possible. We denote this special permeability by $\kappa^S(x)$. We note that we can choose $\kappa^S(x) = \kappa(x;\mu_0)$ as mentioned above. The idea is to construct multiscale basis functions for this permeability and use them as initial basis functions for our construction (Item 6 of the offline stage, Section 3.5.1). Multiscale basis functions solve local problems (see (23) and Section 3.5 where a summary of the method is presented). A good choice of the permeability field κ^S is possible for some problems. We discuss this issue further in the next section.

As an alternative to the multiscale basis functions defined in (23), we can consider energy minimizing basis functions (see [37]), where basis functions are obtained by minimizing the energy of the basis functions subject to a global constraint. More precisely, one can use the partition of unity functions $\{\chi_i^{emf}\}_{i=1}^{N_v}$, with N_v being the number of coarse nodes, that provide the least energy. This can be accomplished by solving

$$\min_{\chi_i^{emf}} \sum_i \int_{\omega_i} \kappa^S |\nabla \chi_i^{emf}|^2 \tag{13}$$

subject to $\sum_i \chi_i^{emf} = 1$ with $\mathrm{Supp}(\chi_i) \subset \omega_i$, $i = 1, \ldots, N_v$. Note that the restriction $\sum_i \chi_i^{emf} = 1$ is a global constraint though it is not tied to any particular global fields.

3.2 Spectral Multiscale basis

The initial coarse basis functions χ_i (discussed above) often need to be complemented if more accurate coarse-scale solutions or more robust preconditioners are sought. This completion is accomplished via local spectral problems. For the case of parameter-dependent elliptic problems considered here, this completion is done at the online stage. See Section 3.5.2. Following [16, 13], we consider, in the online computations, the local parametric homogeneous Neumann eigenvalue problem

$$-\mathrm{div}(\kappa(x;\mu)\nabla\varphi^{\omega_i}(x;\mu)) = \lambda\widetilde{\kappa}(x;\mu)\varphi^{\omega_i}(x;\mu), \tag{14}$$

posed on subdomains ω_i. Here, the modified weight $\widetilde{\kappa}$ is defined by

$$\widetilde{\kappa}(x;\mu) = \frac{1}{H^2}\kappa(x;\mu)\sum_{j=1}^{N_v} |\nabla\chi_j|^2, \tag{15}$$

where χ_j are the initial basis functions.

In this paper, we will use RB techniques to compute cheap online approximations of this eigenvalue problem. The online approximation is computed based on the reduced order model constructed offline.

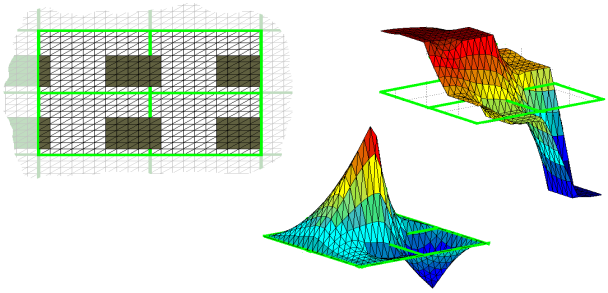

Figure 2: Schematic description of basis function construction. Left: subdomain ω_i. Right-Top: Selected eigenvector φ_i^ℓ with small eigenvalue. Right-Bottom: product $\chi_i\varphi_i^\ell$ where χ_i is the initial basis function of node i.

The construction is summarized in Items 5-9 in Section 3.5.1 and further detailed in Section 3.3 where we describe the RB procedure applied to the eigenvalue problem above. Recall that we denote by

$$\lambda_\ell^{\omega_i,N_{rb}} = \lambda_\ell^{\omega_i,N_{rb}}(\mu) \text{ and } \varphi_\ell^{\omega_i,N_{rb}} = \varphi_\ell^{\omega_i,N_{rb}}(x;\mu)$$

the online RB approximation of the eigenvalue problem (14); see Section 3.5 where a summary of the method is presented. This approximation is computed by solving the small linear system in (24). The RB procedure parameter N_{rb} is introduced in Section 3.5.1. It denotes the number of RB parameter values used for the construction of the reduced order eigenvalue problem. During our online stage (described in Section 3.5.2), we construct multiscale basis functions. The (online) multiscale basis functions are constructed as $\chi_i^\ell = \chi_i^\ell(x;\mu) = \chi_i^*\varphi_\ell^{\omega_i,N_{rb}}$ (see Item 3 of Section 3.5.2 and Figure 2 for illustration). The coarse space is

$$V_0 = V_0(\mu) = \text{span}(\chi_i^*\varphi_\ell^{\omega_i,N_{rb}}).$$

The coarse-scale solution is sought based on (3) with the coarse space above. We note that the local blocks of the coarse matrix (see (7) will be dense due to the fact that local eigenfunctions are supported in the coarse grid block. However, the coarse matrix will have a block sparse structure. The overall sparsity of the blocks of coarse matrix can be increased with a choice of initial multiscale basis functions.

Next, we discuss some properties of the local eigenvalue problem of the fine-scale system. We remind the notation for fine-scale eigenvalues and eigenvectors of the true eigenvalue problem (14)

$$\lambda_\ell^{\omega_i} = \lambda_\ell^{\omega_i}(\mu) \text{ and } \varphi_\ell^{\omega_i} = \varphi_\ell^{\omega_i}(x;\mu).$$

The choice of initial basis functions is important for defining local spectral spaces. We would like to discuss the dimension of the coarse space in the presence of high-conductivity inclusions. For this reason, we assume in the rest of the subsection that the initial multiscale basis function is computed for an online value of the parameter and RB approximation of the local spectral problem is accurate (see discussions later about coarse-space dimension reduction when offline initial multiscale basis functions are used). Assume eigenvalues are given by

$$0 = \lambda_1^{\omega_i} \leq \lambda_2^{\omega_i} \leq ....$$

Basis functions are computed by selecting a number of eigenvalues (starting with small ones) and multiplying corresponding eigenvectors by χ_i (see Figure 2 for the illustration). Thus, the multiscale space is defined for each i as the span of $\chi_i\varphi_\ell^{\omega_i}$, $\ell = 1, ..., L_i$, where L_i is the number of selected eigenvectors. In [16], we show that under some conditions the convergence rate is inversely related to the smallest eigenvalue whose eigenvector is not included in the coarse space. This is also observed in our numerical results. More precisely, we show in [16] that the convergence rate in the energy norm $\int_D \kappa(x;\mu)|\nabla(u-u_0)|^2$ is proportional to

$$\max_i \frac{H^{1+\beta}}{\lambda_{L_i+1}^{\omega_i}}, \tag{16}$$

where H is the coarse mesh size and $\beta \geq 0$ is related to the smoothness of the coefficients. Thus, our goal is to find initial basis functions such that the resulting eigenvalue problem has fewer small eigenvalues.

In high-contrast problems, one can show that the number of small eigenvalues is related to the number of isolated inclusions within a coarse region, see [16, 20]. These contrast-dependent small eigenvalues are inversely proportional to the contrast for the isolated inclusions, and, thus, they can be very small in high-contrast problems. One can show that by using initial multiscale basis functions (see [16, 20]), we can eliminate small inclusions (smaller than the coarse region) by incorporating their effects into one (per coarse node) basis function. As a result, the local spectral problem identifies features that are not included in the initial multiscale space. These features typically consist of high-conductivity channels (channel is a high-conductivity region that connects two boundaries of the coarse region). Thus, it is important to use multiscale basis functions in constructing the weight function in (14). Initial multiscale basis functions will allow achieving smaller dimensional coarse spaces by eliminating many small eigenvalues. In RB-MsFEM, one of our goals is to incorporate small-scale features of the ensemble into multiscale basis functions in order to achieve small dimensional coarse spaces (see Section 4).

3.3 Reduced Basis for eigenvalue problems

The RB method is used to reduce the dimension of the eigenvalue problem so that we can compute the basis functions during the online stage with a much reduced workload. The RB approach, mainly consists of defining a (small) set of functions, denoted by $X_{N_{rb}}$, that can approximate the manifold $\{\varphi_\ell^{\omega_i}(x;\mu)$, with $\varphi_\ell^{\omega_i}$ solution to (21), $\mu \in \Lambda_{trial}\}$. This set is constructed iteratively by a Greedy procedure, which consists of solving the eigenvalue problem for some selected values of the parameter μ. We thus can write

$$X_{N_{rb}} := \text{Span}\left\{\varphi_\ell^{\omega_i}(\mu_m), 1 \leq m \leq N_{rb}, \lambda_\ell^{\omega_i}(\mu_m) \leq \tau\right\}.$$

Once this space is defined, solving (21) for a given value of μ amounts to finding $\left\{\varphi_\ell^{\omega_i,N_{rb}}(\mu), \lambda_\ell^{\omega_i,N_{rb}}(\mu)\right\} \in X_{N_{rb}} \times \mathbb{R}$ such that

$$\forall v \in X_{N_{rb}}, \quad \int_{\omega_i} \kappa(x;\mu)\nabla\varphi_\ell^{\omega_i,N_{rb}}\nabla v dx = \lambda_\ell^{\omega_i,N_{rb}} \int_{\omega_i} \widetilde{\kappa}(x;\mu)\varphi_\ell^{\omega_i,N_{rb}} v dx.$$

In this section, we will discuss the Greedy procedure by itself: how to choose the judicious set of $\{\mu_m\}_{1\leq m\leq N_{rb}}$ and then describe the key element of this procedure which is the error estimate, in the particular case of the linear eigenvalue problem.

The Greedy Algorithm. We would like to choose the set of parameters $\{\mu_m\}_{1\leq m\leq N_{rb}}$ such that it minimizes the error between the solution and its reduced basis approximation, namely $e(\mu) = \|\varphi_\ell^{\omega_i}(\mu) - \varphi_\ell^{\omega_i,N_{rb}}(\mu)\|_{H^1(\omega_i)}$, as a function of μ. In other words, the desirable choice of μ is defined by:

$$\{\mu_m\}_{1\leq m\leq N_{rb}} = \inf_{\{\mu_m\}_{1\leq m\leq N_{rb}}\in\Lambda^{N_{rb}}} \left(\sup_{\mu\in\Lambda} \|\varphi_\ell^{\omega_i} - \varphi_\ell^{\omega_i,N_{rb}}\|_{H^1(\omega_i)}\right).$$

In practice, we don't want to compute $\varphi_\ell^{\omega_i}(\mu), \mu\in\Lambda$ for a twofold reason: first Λ can be a continuous set, second computing $\varphi_\ell^{\omega_i}(\mu)$ for a given μ is computationally expensive, and so we just want to perform this computation for the selected $\{\mu_m\}_{1\leq m\leq N_{rb}}$. Therefore, the RB approach suggests a feasible procedure, which consists of selecting the minimizers of

$$\{\mu_m\}_{1\leq m\leq N_{rb}} = \inf_{\{\mu_m\}_{1\leq m\leq N_{rb}}\in\Lambda_{trial}^{N_{rb}}} \left(\sup_{\mu\in\Lambda_{trial}} \Delta_{N_{rb}}(\mu)\right),$$

where Λ_{trial} is a discrete set and $\Delta_{N_{rb}}(\mu)$ is an estimator of the quantity $e(\mu)$, the choice of which is discussed in the paragraph below. We are now in position to describe the Greedy procedure. We will select the sequence $\{\mu_m\}_{1\leq m\leq N_{rb}}$ incrementally:

1. choose $\mu_1\in\Lambda_{trial}$
2. solve (21) with $\mu=\mu_1$ to define $X_1 := \text{span}\,(\varphi_\ell^{\omega_i}(\mu_1), \lambda_\ell^{\omega_i}(\mu_1)\leq\tau)$,
3. for $m=2$ to N_{rb} do
4. choose $\mu_m := \max_{\mu\in\Lambda_{trial}} \Delta_{m-1}(\mu)$,
5. solve (21) with $\mu=\mu_m$ to define $X_m := \text{span}\,(\varphi_\ell^{\omega_i}(\mu_j), \lambda_\ell^{\omega_i}(\mu_j)\leq\tau, 1\leq j\leq m)$
6. end for

Remark 1. *For numerical reason, it is very important to orthogonalize and normalize the space $X_{N_{rb}}$. It can be achieved by a Gram-Schmidt procedure during the greedy procedure.*

Error estimation for eigenvalue problem. We are thus left with the definition of $\Delta_N(\mu)$. We will use the error estimator introduced in [27]. First, we introduce the weak formulation of the eigenvalue problem:

$$\forall v\in H^1(\omega_i),\quad a_{\omega_i}(\varphi_\ell^{\omega_i}; v;\mu) = \lambda_\ell^i m_{\omega_i}(\varphi_\ell^{\omega_i}, v;\mu),$$

where

$$a_{\omega_i}(u,v;\mu) := \int_{\omega_i}\kappa(x;\mu)\nabla u\cdot\nabla v dx \quad\text{and}\quad m_{\omega_i}(u,v;\mu) := \int_{\omega_i}\widetilde{\kappa}(x;\mu)uv dx.$$

Following [27], we first define a scalar product

$$0<\alpha\leq g(\mu)\underline{a}_{\omega_i}(v,w)\leq a_{\omega_i}(v,w;\mu)$$

and then define (implicitly) $e_N^\ell(\mu)$ as the dual of the residual, namely

$$\forall v\in H^1(\omega_i),\quad \underline{a}_{\omega_i}(e_N^\ell(\mu), v) = a_{\omega_i}(\varphi_\ell^{\omega_i,N}, v;\mu) - \lambda_\ell^{\omega_i,N} m_{\omega_i}(\varphi_\ell^{\omega_i,N}, v;\mu), \tag{17}$$

where $\{\varphi_\ell^{\omega_i,N}, \lambda_\ell^{\omega_i,N}\}$ is the solution to

$$\forall v^N \in X_N, \quad a_{\omega_i}(\varphi_\ell^{\omega_i,N}, v^N; \mu) = \lambda_\ell^{\omega_i,N} m_{\omega_i}(\varphi_\ell^{\omega_i,N}, v^N; \mu).$$

Observe that, due to the linearity of equation (17), the dual of the residual $e_N^\ell(\mu)$ satisfy an affine expansion, similarly to the coefficient $\kappa(x;\mu)$. It reads:

$$e_\ell^N(\mu) = \sum_{q=1}^{Q} \Theta_q(\mu)(e_{\ell,q}^{1,N} - \lambda_\ell^{\omega_i,N}(\mu) e_{\ell,q}^{2,N}),$$

where

$$\underline{a}_{\omega_i}(e_{\ell,q}^{1,N}, v) = a_{\omega_i}^q(\varphi_\ell^{\omega_i,N}, v) \quad \text{and} \quad \underline{a}_{\omega_i}(e_{\ell,q}^{2,N}, v) = m_{\omega_i}^q(\varphi_\ell^{\omega_i,N}, v).$$

We now turn to the definition of the error estimate, Δ_N writes

$$\Delta_N(\mu) := \sum_{\ell=1}^{N_\tau} \frac{\underline{a}_{\omega_i}(e_N^\ell, e_N^\ell)}{\lambda_\ell^{\omega_i,N}},$$

where N_τ is the cardinal of the ensemble $\{\ell \in \mathbb{N}, \lambda_\ell^{\omega_i,N} \leq \tau\}$. We note that this estimator may not be robust for general high-contrast problems; however, we find it to work well for the problems studied numerically in this paper.

Remark 2. *By the definition of the error estimate, we need to solve $2 \times Q$ Poisson problems for each new basis function.*

Remark 3. *Most of the computational efficiency, lies in the fact that $\kappa(x;\mu)$ is an affine representation of the parameter or functionals of the parameter. This affine representation allows us to represent Δ_N as an affine function of μ or functionals of μ and thus to pre-compute all the matrices of its expansion. Affine representation assumption can be relaxed as noted in previous findings, e.g, [6] by representing a general functional dependence via an affine approximation. Another case that is of interest to applied community is when the permeability field is described discretely without any explicit parametrization. In this case, one needs to define affine representation of the permeability field in order to take an advantage of RB framework. Otherwise, the computation of stiffness matrix at the online stage will require the calculations on the fine grid.*

Offline Assemble We take advantage of the affine representation to precompute all stiffness matrices of the coarse scale problem, so that we speed-up the online computation. For this purpose, we need that the the online initial basis function χ_i^* corresponds to the offline partition of unity χ_i.

In our case, we have to pre-compute the following integrals, for all i_1 and i_2, and each ℓ_1 and ℓ_2 and all $1 \leq q \leq Q$ and all $1 \leq m_1, m_2 \leq N_{rb}$, compute:

$$K_q(i_1, \ell_1, i_2, \ell_2, m_1, m_2) := \int_D k_q(x) \nabla \left(\chi_{i_1} \varphi_{\ell_1}^{\omega_{i_1}}(\mu_{m_1})\right) \nabla \left(\chi_{i_2} \varphi_{\ell_2}^{\omega_{i_2}}(\mu_{m_2})\right). \tag{18}$$

Then, during the online computations, once we solve the reduced order local spectral problem:

$$\forall v \in X_{N_{rb}}, \quad \int_{\omega_i} \kappa(x;\mu) \nabla \varphi_\ell^{\omega_i,N_{rb}} \nabla v dx = \lambda_\ell^{\omega_i,N_{rb}} \int_{\omega_i} \widetilde{\kappa}(x;\mu) \varphi_\ell^{\omega_i,N_{rb}} v dx$$

and obtain the following representation of $\varphi_\ell^{\omega_i,N_{rb}}$ as a linear combination of the vector field in $X_{N_{rb}}$:

$$\varphi_\ell^{\omega_i,N_{rb}} := \sum_{m=1}^{N_{rb}} \sum_{j=1}^{N_\tau(\mu_m)} \alpha_{mj}(\mu)\varphi_j^{\omega_i}(\mu_m).$$

We can construct the coarse stiffness matrices, using pre-computed matrices:

$$K_{coarse} := \sum_{q=1}^{Q} \sum_{(m_1,m_2)=1}^{N_{rb}} \sum_{j_1=1}^{N_\tau(\mu_{m_1})} \sum_{j_2=1}^{N_\tau(\mu_{m_2})} \Theta_q(\mu)\alpha_{m_1 j_1}\alpha_{m_2 j_2} K_q(i_1,\ell_1,i_2,\ell_2,m_1,m_2).$$

3.4 Online computation

In the online stage, we first compute on each coarse region ω_i the reduced eigenvalue problem, and then define the multiscale basis functions

$$\chi_i^\ell := \chi_i \varphi_\ell^{\omega_i,N_{rb}}.$$

We then assemble the coarse-grid problem, using the precomputed matrices (if χ_i is independent of μ). With a reduced-dimensional eigenvalue problem, we can rapidly solve the local spectral problem and construct multiscale basis functions. These basis functions are further used to solve the global problem. This approach can be effectively used when the parameter μ is a coarse-grid spatial function, i.e., μ varies on a coarse grid where the parameter in each coarse block is assumed to be an independent scalar quantity. In this case, one has a very large dimensional parameter space, and approaches such as the ones proposed in this paper are needed for efficient computations because local problems will involve only a scalar parameter. RB-MsFEM allows rapidly computing the global solution.

We note that the coarse-scale system obtained by solving reduced eigenvalue problems will have the same dimension as the coarse-scale system where the the exact eigenvalue problem is solved (i.e., they have the same number of important eigenvalues). The computational saving is due to solving small-size local eigenvalue problems. As we noted earlier, the eigenvalue problem can have a large dimension and thus the basis function can be expensive for each value of μ. Using the RB, we simplify these computations.

As we noted that these coarse spaces can be used for designing preconditioners. In particular, one can use the coarse spaces computed with the RB in two-level additive Schwarz preconditioners

$$B^{-1}(\mu) = (R_0^{RB}(\mu))^T (A_0^{RB}(\mu))^{-1} R_0^{RB}(\mu) + \sum_{i=1}^{N} R_i(\mu)^T A_i^{-1}(\mu) R_i(\mu), \tag{19}$$

where R_0 and A_0 are defined using the coarse space computed online. The local matrices $A_i(\mu)$ correspond to the exact local solver for each μ as in the standard two-level additive Schwarz constructed for (9). The computations of the latter involve local corrections while the former requires local eigenvalue computations and downscaling operators that are computed using the reduced system. We will show numerically that these preconditioners are optimal with respect to the contrast, i.e., $cond(B^{-1}(\mu)A(\mu))$ is bounded independent of the contrast.

We can use inexact local solvers instead of exact solvers $A_i(\mu)^{-1}$ in subdomains ([35]). In our proposed methods, the inexact solvers can be constructed rapidly at the online stage via pre-computed calculations from the offline stage. The offline stage will involve RB technique for identifying important Dirichlet modes of local problems and downscaling operators. This information can be used to construct inexact solver

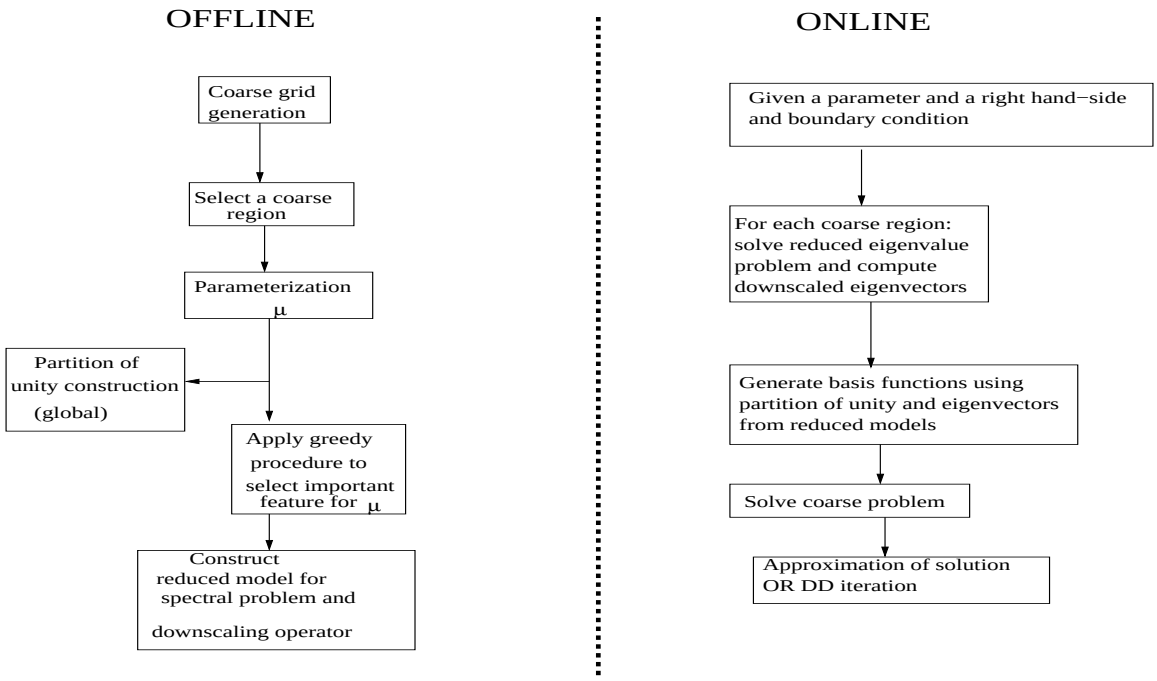

Figure 3: Flow chart

approximation. The required properties for these inexact solvers that will guarantee robust preconditioners can be found in, e.g., [35].

3.5 Description of the algorithm

In this section, we summarize the algorithm. We present an overall picture of all the computations involved. We distinguish the following computations.

- Offline computation (Section 3.5.1):
  - Coarse grid generation and parameter set discretization;
  - Computation of the initial partition of unity;
  - Individual subdomain RB computations to construct reduced order models for subdomain parametric eigenvalue problems.
- Online computations (Section 3.5.2):
  - Individual computation of reduced order eigenvalue problems for given parameter value;
  - Construction of coarse spaces with important modes;
  - Approximation of solutions using the coarse spaces.

A schematic description of the algorithm is presented in Figure 3. Itemized step-by-step more precise descriptions of the computations are presented in Section 3.5.1 and 3.5.2 below. Further details related to the design and analysis of some individual steps were presented in previous sections.

3.5.1 Offline stage

We assume here that a fine grid, on which κ is defined, is given. We also assume that we know the parameter space $\mu \in \Lambda \subset \mathbb{R}^d$, a threshold τ and a number N_{rb}, that corresponds to the the number of selected parameter value. We then proceed as follows:

1. Define a coarse mesh $\mathcal{T}_H$ and the $\mathbb{P}_1$ finite element basis functions $W_H = \text{Span}\left\{\chi_i^0\right\}$,
2. Define Λ_{trial} as a discrete subset of Λ,
3. Choose a partition of unity $\{\chi_i\}_{1\leq i\leq N_v}$. We can choose the linear basis function (χ_i^0), but other choices can be made (see Section 3.2)
4. For each coarse region ω_i,
5. Compute on the fine grid the following stiffness and mass matrices for all $1 \leq q \leq Q$

$$v^T A_q^{\omega_i} u := \int_{\omega_i} \kappa_q(x) \nabla u \cdot \nabla v dx \quad \text{and} \quad v^T M_q^{\omega_i} u := \int_{\omega_i} \kappa_q(x) \sum_{k=1}^{N_v} |\nabla \chi_k|^2 \, uv dx. \tag{20}$$

6. Define the sequence $\{\mu_m\}_{1\leq m\leq N_{rb}}$, using a Greedy procedure (see Section 3.3 below), and solve

$$\sum_{q=1}^{Q} \Theta_q(\mu_j)(A_q^{\omega_i} - \lambda_\ell^{\omega_i}(\mu_m) M_q^{\omega_i}) \varphi_\ell^{\omega_i}(\mu_m) = 0, \quad \lambda_\ell^{\omega_i}(\mu_m) \leq \tau. \tag{21}$$

7. Construct the matrix

$$R_{\omega_i}^T := [\varphi_\ell^{\omega_i}(\mu_m), \lambda_\ell^{\omega_i}(\mu_m) \leq \tau, 1 \leq m \leq N_{rb}]. \tag{22}$$

8. end for
9. Outputs of the offline stage are R_{ω_i}, $A_j^{\omega_i}$, $M_j^{\omega_i}$ and $R_0^T := [\chi_i, 1 \leq i \leq N_v]$

Remark 4. *Note that a possible choice for the partition of unity, is to select a judicious value of μ_0 (see discussions later on selecting multiscale basis functions) and for each element $K_i \in \mathcal{T}_H$ compute the following* multiscale *partition of unity functions:*

$$-div\left[(\kappa(x;\mu_0))\,\nabla\chi_i(x)\right] = 0 \text{ in } K_i, \quad \chi_i = \chi_i^0 \text{ on } \partial K_i. \tag{23}$$

3.5.2 Online stage

The purpose of this step is to compute the solution for a given value of μ and a given f:

1. For each coarse region ω_i
2. Solve the reduced order eigenvalue problem and keep only some eigenvectors that correspond to eigenvalues below a certain threshold

$$\sum_{q=1}^{Q} \Theta_q(\mu) \left(R_{\omega_i}^T A_q^{\omega_i} R_{\omega_i} - \lambda_\ell^{\omega_i, N_{rb}}(\mu) R_{\omega_i}^T M_q^{\omega_i} R_{\omega_i} \right) \varphi_\ell^{\omega_i, N_{rb}}(\mu) = 0, \quad \lambda_\ell^{\omega_i, N_{rb}}(\mu) \leq \tau. \tag{24}$$

3. Compute the multiscale basis functions (see Section 3.2 below)

$$\chi_i^j := \chi_i^* \varphi_j^{\omega_i, N_{rb}}.$$

4. end for

5. Solve the coarse-grid system and use it in two-level preconditioners (if needed).

Remark 5. *Note that the standard choice of initial basis functions χ_i^* is the partition of unity used during the offline stage χ_i, but other choices can be employed. For instance, we can choose to compute online partition of unity for the given value of μ (See Section 4).*

Remark 6. *We note that our proposed method can be extended to time-dependent parabolic equations, $\frac{\partial u}{\partial t} - div(\kappa(x;\mu)\nabla u) = f$, or some other model problems. In this case, the offline part of the algorithm will remain the same and involve multiscale basis function computations via local eigenvalue problems and RB procedure. In the online stage, the computation of online coarse space V_0 will also remain unchanged. However, the coarse-grid global problem formulation will change to*

$$\left(\frac{\partial u_0}{\partial t}, v\right) - a(u_0, v; \mu) = f(v), \quad \text{for all } v \in V_0, \tag{25}$$

where $(\cdot,\cdot)$ is the usual L_2 inner product,

$$a(u, v; \mu) = \int_D \kappa(x;\mu)\nabla u(x)\nabla v(x)dx \quad \text{for all } u, v \in H_0^1(D) \tag{26}$$

and $f(v) = \int_D f(x)v(x)dx$ for all $v \in H_0^1(D)$. One can solve (25) implicitly on a coarse grid. Because multiscale basis functions do not change in time, this will provide additional CPU savings.

4 Numerical results and discussions

In this section, we present representative numerical results for the coarse-scale approximation with the RB and its use in two-level additive preconditioners. The equation $-\text{div}(\kappa(x;\mu)\nabla u) = 1$ is solved with boundary conditions $u = x + y$ on ∂D. For the coarse-scale approximation, we will vary the dimension of the coarse spaces (online) and change offline space dimensions. We will investigate the convergence rate as a function of minimum eigenvalue and the contrast. For preconditioning results for (9), we will investigate the behavior of the condition number of $B^{-1}(\mu)A(\mu)$, where $B^{-1}(\mu)$ is defined in (19), as we increase the contrast for various choices of coarse spaces that include variations in online and offline parameter setting. In our simulations, we run the Preconditioned Conjugate Gradient (PCG) until the ℓ_2 norm of the residual is reduced by a factor of 10^{10}. We take $D = [0,1] \times [0,1]$ that is divided into 5×5 (example 1) or 8×8 (example 2) equal square subdomains. Inside each subdomain we use a fine-scale triangulation, where triangular elements constructed from 10×10 squares are used. The size of the fine-scale mesh is denoted by h.

In our numerical experiments, we test the accuracy of RB-MsFEMs when coarse spaces include eigenvectors corresponding to small, asymptotically vanishing (as contrast increases), eigenvalues as well the cases when additional eigenvectors are included in the coarse space (see [16] for more discussions). We choose the following notation: LSM+n indicates that the coarse spaces include eigenvectors corresponding to small,

asymptotically vanishing as contrast increases, eigenvalues and an additional n eigenvectors corresponding to the next n eigenvalues (in an increasing order). E.g., LSM+0 indicates the coarse space that only includes eigenvectors corresponding to small, asymptotically vanishing eigenvalues, while LSM+1 indicates the coarse space that includes eigenvectors corresponding to small, asymptotically vanishing eigenvalues, plus one more eigenvector in each coarse region that corresponds to the next largest eigenvalue. We consider two different contrasts. We study the convergence of the methods LSM (when χ^0 are used to compute $\widetilde{\kappa}$ and then $\widetilde{\kappa} \approx \kappa$) and $\widetilde{\text{LSM}}$ (when multiscale basis functions χ^{ms}, see (23), are used to construct $\widetilde{\kappa}$). We will consider the error in the following energy norm

$$e_A := \|u - u_{ref}\|_A^2 / \|u_{ref}\|_A^2,$$

where

$$\|u\|_A^2 = \int_D \kappa(x;\mu) \left|\nabla u(x)\right|^2 dx.$$

We implement a two-level additive preconditioner with the following coarse spaces: multiscale functions with linear boundary conditions (MS); spectral coarse spaces with $\widetilde{\kappa} = \kappa$ where piecewise linear partition of unity functions are used as an initial space (LSM $\widetilde{\kappa} \approx \kappa$).

In the first numerical example, we consider a permeability field which is the sum of two permeability fields with each containing inclusions such that their sum gives a channelized permeability field. The permeability field is described by

$$\kappa(x;\mu) := (1-\mu)\kappa_0(x) + \mu\kappa_1(x).$$

We can represent 3 distinct different features in $\kappa(x;\mu)$: inclusions (left), channels (middle), and shifted inclusions (right), see Figure 4. We note that the other permeability fields introduce some connection between the inclusions. There exists no single value of μ that has all the features. Furthermore, we will use a trial set for the reduced basis algorithm that does not include $\mu = 0.5$. Our goal is to show that the proposed techniques are accurate and robust with respect to the parameter and the contrast. We will not present convergence results in terms of discretization parameters.

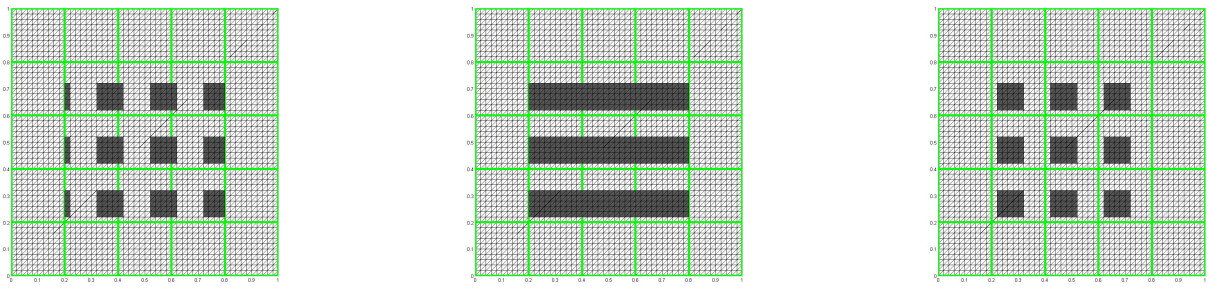

Figure 4: From left to right: $\mu = 0$, $\mu = 1/2$ and $\mu = 1$.

As there are three distinct spatial fields in the space of conductivities, we will choose several functions (between one to four) in our reduced basis set to represent the manifold for μ. In the cases of one and two

$H = 1/5$	true	$N_{rb} = 1$	$N_{rb} = 2$	$N_{rb} = 3$	$N_{rb} = 4$
LSM+0	13.58(44)	39.22(36)	39.22(36)	13.58(44)	13.58(44)
LSM+1	4.01(80)	36.75(72)	27.59(72)	4.01(80)	4.01(80)
LSM+2	3.93(116)	34.65(108)	28.06(108)	3.93(116)	3.93(116)

Table 1: Convergence results (energy norm in % and space dimension) for RB-MsFEM with the increasing dimension of the coarse space. LSM+n indicates that the coarse spaces include eigenvectors corresponding to small, asymptotically vanishing eigenvalues, and additional n eigenvectors corresponding to the next n eigenvalues. Here, $\eta = 10^4$. $\mu = 1/2$ (error with MsFEM 39.07%).

$H = 1/5$	true	$N_{rb} = 1$	$N_{rb} = 2$	$N_{rb} = 3$	$N_{rb} = 4$
LSM+0	13.61(44)	39.30(36)	39.30(36)	13.61(44)	13.61(44)
LSM+1	4.01(80)	39.29(72)	38.65(72)	4.01(80)	4.01(80)
LSM+2	3.93(116)	39.18(108)	26.48(108)	3.93(116)	3.93(116)

Table 2: Convergence results (energy norm in % and space dimension) for RB-MsFEM with the increasing dimension of the coarse space. LSM+n indicates that the coarse spaces include eigenvectors corresponding to small, asymptotically vanishing eigenvalues, and additional n eigenvectors corresponding to the next n eigenvalues. Here, $\eta = 10^6$. $\mu = 1/2$ (error with MsFEM 39.29%).

permeability fields, we will observe that when the online permeability field does not contain appropriate features, then we can not obtain the convergence. Note that the greedy procedure selects the number of dimension of the reduced space in terms of the parameter while the number of small eigenvalues controls the number of basis functions at the online stage. We observe in Tables 1-4 that we indeed need $N_{rb} \geq 3$ to capture all the details of the solution. In these tables, we compare the errors obtained with RB-MsFEM when the online problem is solved with a corresponding number of basis functions. We observe a convergence with respect to the number of local eigenvectors when N_{rb} is chosen such that it contains spatial features included in the conductivity space. In particular, we observe that the error is comparable to the error of "true" - when the online multiscale basis functions and local spectral problems are solved for the online value of μ. However, the cost of the computations at the online stage is substantially lower when RB is utilized. We have also computed weighted L_2 error which shows a similar trend and these errors are much lower (typically less than 2 %). Some numerical illustrations are depicted in Figure 5 where we plot the fine-scale solution (top left), the solution computed with one multiscale basis functions computed for the online value of μ (top right), the solution computed with RB-MsFEM (bottom left), and the solution computed with the spectral multiscale method (bottom right) where the initial partition of unity and the local spectral problem are solved for the online value of μ. We see from this figure that RB-MsFEM provides a solution that is close to the true, fine-scale, solution.

We use the same example as before for testing the two-level additive Schwarz preconditioners. In this example, we only use coarse spaces based on reduced models. The numerical results are presented in Tables 5-8. In these numerical results, we observe that when the dimension of the reduced space is 3 and more, the condition number of the preconditioned system is independent of the contrast. In all these examples, we only choose the eigenvectors that correspond to eigenvalues that are small and asymptotically vanishing. Note that in this example, we only choose basis functions corresponding to the interior nodes, while in

$H = 1/5$	true	$N_{rb} = 1$	$N_{rb} = 2$	$N_{rb} = 3$	$N_{rb} = 4$
LSM+0	9.92(80)	92.56(36)	50.73(68)	9.85(80)	9.90(80)
LSM+1	3.19(116)	89.93(72)	20.65(112)	3.48(116)	3.48(116)
LSM+2	3.06(152)	88.76(108)	3.85(150)	3.06(152)	3.07(152)

Table 3: Convergence results (energy norm in % and space dimension) for RB-MsFEM with the increasing dimension of the coarse space. LSM+n indicates that the coarse spaces include eigenvectors corresponding to small, asymptotically vanishing eigenvalues, and additional n eigenvectors corresponding to the next n eigenvalues. Here, $\eta = 10^4$. $\mu = 1$ (error with MsFEM 48.87%).

$H = 1/5$	true	$N_{rb} = 1$	$N_{rb} = 2$	$N_{rb} = 3$	$N_{rb} = 4$
LSM+0	9.95(80)	92.73(36)	51.29(74)	9.93(80)	9.93(80)
LSM+1	3.19(116)	92.73(72)	14.88(112)	3.48(116)	3.48(116)
LSM+2	3.06(152)	92.63(108)	21.14(150)	3.06(152)	3.08(152)

Table 4: Convergence results (energy norm in % and space dimension) for RB-MsFEM with the increasing dimension of the coarse space. LSM+n indicates that the coarse spaces include eigenvectors corresponding to small, asymptotically vanishing eigenvalues, and additional n eigenvectors corresponding to the next n eigenvalues. Here, $\eta = 10^6$. $\mu = 1$ (error with MsFEM 49.09%).

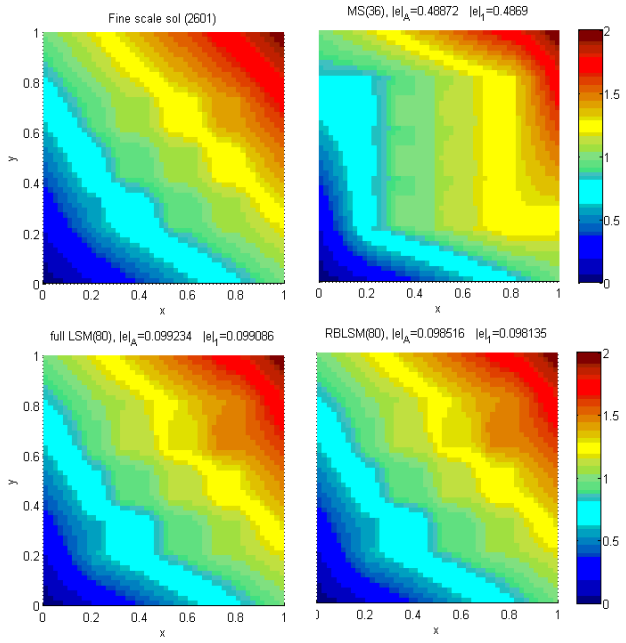

Figure 5: Contrast $\eta = 10^4$, $\mu = 1$, $N_{rb} = 3$, LSM+0.

the coarse-grid approximation, we choose basis functions that also represent boundary nodes. We observe that the number of iterations does not change as the contrast increases when spectral coarse spaces are used. On the contrary, when using multiscale basis functions (one basis per coarse node), the condition number of the preconditioned matrix increases as the contrast increases. The latter is due to the fact that the coarse space does not contain enough degrees of freedom.

η	MS	true	$N_{rb}=1$	$N_{rb}=2$	$N_{rb}=3$	$N_{rb}=4$
10^5	$47(1.36e+004)$	$27(8.69e+000)$	$42(2.02e+004)$	$45(1.75e+004)$	$26(9.34e+000)$	$26(9.34e+000)$
10^7	$57(1.36e+006)$	$31(7.81e+000)$	$52(2.02e+006)$	$53(2.02e+006)$	$28(9.34e+000)$	$28(9.34e+000)$
Dim	16	24	16	16	24	24

Table 5: Number of iterations until convergence and estimated condition number for the PCG and different values of the contrast η with $\mu = 1/2$. We set the tolerance to 1e-10. Here $H = 1/5$ with $h = 1/50$.

η	MS	true	$N_{rb}=1$	$N_{rb}=2$	$N_{rb}=3$	$N_{rb}=4$
10^5	$24(1.18e+001)$	$27(7.81e+000)$	$27(9.37e+000)$	$28(8.08e+000)$	$24(6.16e+000)$	$24(6.16e+000)$
10^7	$25(1.18e+001)$	$27(8.70e+000)$	$27(9.37e+000)$	$29(8.03e+000)$	$28(6.16e+000)$	$28(6.16e+000)$
Dim	16	24	16	34	36	36

Table 6: Number of iterations until convergence and estimated condition number for the PCG and different values of the contrast η with $\mu = 0$. We set the tolerance to 1e-10. Here $H = 1/5$ with $h = 1/50$.

η	MS	true	$N_{rb}=1$	$N_{rb}=2$	$N_{rb}=3$	$N_{rb}=4$
10^5	$27(1.58e+001)$	$29(7.81e+000)$	$34(1.01e+001)$	$28(5.88e+000)$	$28(5.88e+000)$	$27(5.88e+000)$
10^7	$27(1.58e+001)$	$29(7.81e+000)$	$35(1.01e+001)$	$30(5.87e+000)$	$27(5.87e+000)$	$27(5.87e+000)$
Dim	16	60	40	60	60	60

Table 7: Number of iterations until convergence and estimated condition number for the PCG and different values of the contrast η with $\mu = 1$. We set the tolerance to 1e-10. Here $H = 1/5$ with $h = 1/50$.

In the second example, we would like to discuss how a good choice of initial multiscale basis functions will allow achieving a dimension reduction. Indeed, via initial multiscale basis functions, we can incorporate features that can be localized into the initial multiscale basis functions. This property of initial multiscale basis functions works well when the initial partition of unity is computed based on the online value of μ. However, this can be expensive and we attempt to find initial multiscale basis functions that can allow achieving a dimension reduction. This is not always possible as will be argued later on. But we can achieve this if we can construct initial multiscale spaces such that they span all inclusions that are in permeability fields of $\kappa(x;\mu) = \mu\kappa_0(x) + (1-\mu)\kappa_1(x)$. In the permeability field shown in Figure 7, one can construct initial multiscale basis functions that incorporate all features that can be localized. We will use the largest value of μ to construct initial basis function. With these basis functions, we can localize all isolated inclusions of $\kappa(x;\mu)$ that comes from $\kappa_1(x)$ and thus achieve a dimension reduction. Next, we demonstrate numerical results for RB-MsFEM in Tables 9 and 10 for two different contrasts $\eta = 10^4$ and $\eta = 10^6$. One can observe from this table the use of initial multiscale basis functions allows achieving a dimension

η	MS	true	$N_{rb}=1$	$N_{rb}=2$	$N_{rb}=3$	$N_{rb}=4$
10^5	$48(1.16e+004)$	$27(8.69e+000)$	$44(1.86e+004)$	$45(1.62e+004)$	$26(9.34e+000)$	$26(9.34e+000)$
10^7	$57(1.16e+006)$	$29(8.70e+000)$	$52(1.86e+006)$	$54(1.86e+006)$	$28(9.34e+000)$	$28(9.34e+000)$
Dim	16	24	16	16	24	24

Table 8: Number of iterations until convergence and estimated condition number for the PCG and different values of the contrast η with $\mu = 1/3$. We set the tolerance to 1e-10. Here $H = 1/5$ with $h = 1/50$.

$H = 1/8$	RB-LSM	RB-$\widetilde{LSM}$
LSM+0	11.85(156)	13.61(122)
LSM+1	4.68(237)	3.86(203)

Table 9: Convergence results (energy norm in % and space dimension) for RB-MsFEM with the increasing dimension of the coarse space. LSM+n indicates that the coarse spaces include eigenvectors corresponding to small, asymptotically vanishing eigenvalues, and additional n eigenvectors corresponding to the next n eigenvalues. Here, $\eta = 10^4$. $\mu = 1/2$ and $N_{rb} = 3$ (error with MsFEM 21.05%).

reduction for the coarse space without sacrificing the accuracy much. In particular, we achieve a similar error for the coarse spaces with the dimension that is smaller thanks to a good choice of initial multiscale basis functions. Some numerical illustrations are plotted in Figure 7 where we plot the fine-scale solution (top left), the solution computed with one multiscale basis function computed for the online value of μ (top right), the solution computed with RB-MsFEM with piecewise linear initial partition of unity (bottom left), and the solution computed RB-MsFEM with multiscale initial partition of unity (bottom right). We see from this figure that RB-MsFEM with initial multiscale basis functions (with smaller dimensional coarse space) provides a solution that is close to the true, fine-scale, solution. Similar observations can be made for two-level preconditioners.

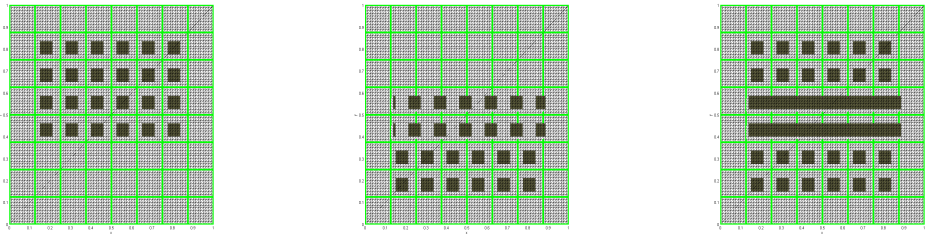

Figure 6: From left to right: $\mu = 0$, $\mu = 1$, and $\mu = 1/2$

Next, we would like to discuss possible estimates for N_{rb} and the choice of initial basis functions for more general setup when the permeability has an affine representation and each $\kappa_i(x)$ is a high-contrast permeability field. In general, it may be difficult to estimate N_{rb} because one needs to identify distinct permeability features in the family $\kappa(x;\mu)$. For example, in our first example, there were three distinct permeability fields in $\kappa(x;\mu)$. In general, we will need to find out which high-conductivity regions of $\kappa_i(x)$

$H = 1/8$	RB-LSM	RB-$\widetilde{LSM}$
LSM+0	11.87(156)	13.59(122)
LSM+1	4.69(237)	3.84(203)

Table 10: Convergence results (energy norm in % and space dimension) for RB-MsFEM with the increasing dimension of the coarse space. LSM+n indicates that the coarse spaces include eigenvectors corresponding to small, asymptotically vanishing eigenvalues, and additional n eigenvectors corresponding to the next n eigenvalues. Here, $\eta = 10^6$. $\mu = 1/2$ and $N_{rb} = 3$ (error with MsFEM 21.16%).

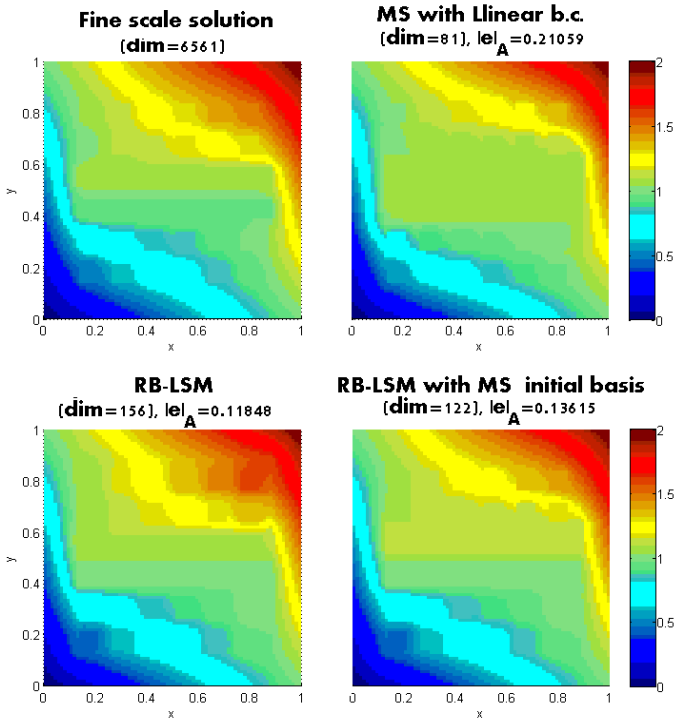

Figure 7: Contrast $\eta = 10^4$, $\mu = 1$, $N_{rb} = 3$, LSM+0

$(i = 1, ..., Q)$ can form channels in $\kappa(x; \mu)$ and how many combinations of these channels can be formed. For example, if we take $\kappa_1(x)$ to have inclusions, while $\kappa_2(x)$,..., $\kappa_Q(x)$ contain inclusions such that each $\kappa_1(x) + \kappa_j(x)$ $(j \neq 1)$ form channels where these channels are not contained in any other combination of $\kappa_1(x) + \kappa_i(x)$, $i \neq j$. In this case, N_{rb} will be of order of Q because each $\kappa_1(x) + \kappa_j(x)$ along with $\kappa_i(x)$ will have distinct high-conductivity features. In general, channels can have complex structures and these connected features may be localized to coarse regions. An initial multiscale basis functions can incorporate some of these features and reduce the dimension. An advantage of the proposed method is that it can identify an appropriate number of representative functions and, consequently estimate N_{rb}, as our numerical results show.

4.1 Discussions on the accuracy of RB-MsFEM

For the accuracy of our approach, we need to include essential features of the parameter-dependent solution space. For this reason, we need to choose (1) an appropriate N_{rb} and (2) the appropriate number of local eigenfunctions and (3) appropriate initial multiscale basis functions. As for initial multiscale basis functions, we would like to include all localizable features across the whole range of the parameter space. As we noted this is not always possible. The error in the proposed approaches will be controlled by the dimension of the coarse space (which includes the number of eigenfunctions we choose and the initial multiscale space) and the number of the reduced space N_{rb}.

When parametrized permeability fields consist of a linear combination of distinct spatial fields that contain channels and inclusions, we can give some insight into the convergence of the method. In this case, for the initial multiscale space, one needs to choose functions that contain small-scale inclusions (that are included within the coarse-grid block) of all permeability fields in the space (c.f., the second numerical example). This can be easily done when $\kappa_q(x)$ contains distinct inclusions and any $\kappa(x; \mu)$ contains some of these inclusions. In this case, we need to choose initial multiscale basis functions such that they include all inclusions (within coarse regions). As for the number of local eigenfunctions, we need to choose all small eigenfunctions in the space and, with appropriate choice of initial multiscale space, the final dimension of the coarse space can be reduced. As for the number of N_{rb}, one needs to choose all distinct important features. E.g., in the first numerical example, we had three distinct spatial fields and the others can be approximated as our numerical results showed.

There is a trade-off in the accuracy of the coarse-grid approximation (the number of eigenvectors chosen to form the coarse space) and the approximation that is due to the selection of appropriate dimension of reduced space (denoted by N_{rb}). This can be observed in our numerical results. E.g., we observe from Table 3, the accuracy with LSM+2 for $N_{rb} = 2$ is about the same as that with LSM+1 for $N_{rb} = 3$. We note that the accuracy of the coarse-grid approximation for an online μ is given by H^γ/λ^*_{L+1}, where λ^*_{L+1} is the smallest of all the eigenvalues (over all coarse regions) that are not included in the coarse space. The next approximation is due to the approximation of the coarse solution for the online parameter value. The error in this approximation is due to the dimension of the reduced space (denoted by N_{rb}). These two errors may be comparable for some cases and one needs to control both errors to achieve a desirable tolerance. For example, if the desired error threshold is large, then one does not need many eigenvectors to include in the coarse space and N_{rb} can be kept low.

4.2 Reduced Basis for the partition of unity

It is possible to use the RB method for the partition of unity function. The main idea is the following. We still pick a μ_0 in the offline stage to define $\widetilde{\kappa}$. We also define a reduced order model for the multiscale basis function, so that we are able to use an *adapted* partition of unity when we define the multiscale basis function in the online stage. For that purpose, we first need to rewrite the problem (23), in a reduced basis manner. Introduce $\phi_i := \chi_i - \chi_i^0$, that solves

$$-\text{div}\left[(\kappa(x;\mu_0))\,\nabla\phi_i(x)\right] = \text{div}\left[(\kappa(x;\mu_0))\,\nabla\chi_i^0(x)\right] \text{ in } K_i, \quad \phi_i = 0 \text{ on } \partial K_i.$$

The weak formulation of this problem can be written as

$$\sum_{q=1}^{Q} \Theta_q(\mu)\left(a_{K_i}^q(\phi_i, v) - b_q(v)\right) = 0,$$

where

$$a_{K_i}^q(u,v) := \int_{K_i} \kappa_q \nabla u \cdot \nabla v \quad \text{and} \quad b_q(v) := \int_{K_i} \kappa_q \nabla\chi_i^0 \cdot \nabla v.$$

Next, we define some key ingredients of the greedy procedure. As in Section 3.3, this is an iterative procedure that selects judicious $\{\mu_j\}_{1\leq j\leq N_{rb}}$ used for the definition of the space $X_{N_{rb}} := \text{span}\,(\phi_i(\mu_j), 1 \leq j \leq N_{rb})$. Suppose that we have already defined N value of μ and therefore the space $X_N = \text{span}\,(\phi_i(\mu_j), 1 \leq j \leq N)$. We now want to find $\mu_{N+1} := \max_{\mu}(\Delta_N(\mu))$. First, we introduce the residual as

$$\forall v \in H^1(K_i), \quad r_N(v;\mu) = \sum_{q=1}^{Q} \Theta_q(\mu)\left(a_{K_i}^q(\phi_i^N, v) - b_q(v)\right),$$

where ϕ_i^N, with obvious notation, is the solution to

$$\forall v \in X_N, \quad \sum_{q=1}^{Q} \Theta_q(\mu)\left(a_{K_i}^q(\phi_i^N, v) - b_q(v)\right) = 0.$$

We then use the classical estimator for the RB method:

$$\Delta_N := \|e_N(\mu)\|_{H^1(K_i)},$$

where e_N is implicitly defined by

$$\forall v \in H^1(K_i), \quad (e_N(\mu), v)_{H^1(K_i)} = r_N(v;\mu).$$

The efficiency of such an approach has been already tested in a different context by [8].

4.3 Computational cost

In this section, we will compare the cost of our approach with the cost of using standard RB method, which consists of using RB method for the problem (1) directly. Here we suppose that (1) the problem

in Eq. (1) can be solved directly (note high condition number problem due to high contrast, and highly detailed mesh due to small length scales in the coefficient) and (2) we do not consider the cost of the offline computation and (3) we ignore the fact that we want to solve this problem for many right-hand side. All these issues are main concerns when using directly the RB method to solve (1), while our approach is designed to circumvent these difficulties. We discuss in the sequel that in the online stage we still speed-up the computation. This is due to the fact that localization allows to separate the inversion of a full matrix, by the inversion of many smaller (full) matrices (this step can be computed in parallel) and the inversion of a sparse matrix (this can be done very efficiently) in our algorithm.

The main computational gain is due to the fact that at the online stage, we do not need all the features that are in global solutions as in standard RB methods. Via local solutions and online basis computations, we can identify small dimensional coarse spaces that are needed to compute the solution at the online stage without sacrificing the accuracy. We note that local computations can be performed in parallel and thus the computational time of solving local problems will be equivalent to that of solving one local problem. Moreover, the coarse problem is sparse, while the standard RB technique will yield a dense system for finding the solution.

Next, we discuss the computational cost. Assume that there are M coarse nodes. For each coarse region, we have at most k important local eigenvectors that represent all essential features of the solution space. Then, at the online stage, for each μ and in each coarse region, we solve a $k \times k$-size eigenvalue problem to identify basis functions. If we choose only a few basis functions for a particular μ, the cost of solving the local eigenvalue problem will scale as k^2 (for simplicity, we assume we have chosen one basis function per coarse node). Moreover, these computations can be performed in parallel. To solve the linear problem defined on a coarse grid, the number of operations will scale as M^2 ($M \times M$ sparse matrix is solved). The total cost for our procedure will scale as $M^2 + Mk^2$. In general, if there are only k_0 eigenvectors per coarse region selected to form multiscale basis functions, then the computational cost is $(k_0 M)^2 + M k_0 k^2$.

To discuss the computational cost of the RB that uses global snapshots, we assume that there are L snapshots of global solutions, $u^{(1)} = (u_1^{(1)}, ..., u_{mM}^{(1)})$,..., $u^{(L)} = (u_1^{(L)}, ..., u_{mM}^{(L)})$ that are selected, where M is the number of coarse nodes and m is the number of fine nodes within a coarse region containing a coarse node. We assume these regions are non-overlapping. The space of these global solutions has a smaller dimension as discussed above. In particular, we assume that the restriction of the solution to a coarse region i, that is spanned by $\xi_i^{(1)} = (u_{(i-1)m+1}^{(1)}, ..., u_{im}^{(1)})$,..., $\xi_i^{(L)} = (u_{(i-1)m+1}^{(L)}, ..., u_{im}^{(L)})$, $i = 1, ..., M$, has the effective dimension k. We assume that the space span$(\xi_i^{(1)}, ..., \xi_i^{(L)})$, that has the dimension k, is spanned by $\zeta_i^{(1)}$, ..., $\zeta_i^{(k)}$. Consequently, the space of solutions $u^{(1)}$, ..., $u^{(L)}$ can be spanned by $\Theta_{(i)}^{(j)} = (0.., 0, \zeta_i^{(j)}, 0, ..., 0)$, $i = 1, ..., M$, $j = 1, ..., k$. Thus, the effective dimension of global snapshots is kM. The Galerkin projection onto this space involves solving $(kM) \times (kM)$ dense matrix system, and thus the work is $(kM)^2$. On the other hand, when using our proposed approach, we solve $(k_0 M) \times (k_0 M)$ sparse matrix system where one can achieve $k_0 M$ computational cost if an optimal solver is employed.

Our proposed procedure will be more efficient for a large number of k's and when only a few of these local features are needed at the online stage, i.e., k_0 is smaller than k. Our proposed approach also becomes more efficient for large values of M, and when the problem is solved multiple times for different right hand sides. Moreover, the computations of our procedure involve sparse matrix computations and can have high parallel efficiency.

5 Conclusions

In this paper, we propose an efficient approach for solving the parameter-dependent multiscale elliptic equation. In our approach, local reduced approximations are used to generate local multiscale basis functions. The local problem setup combines techniques from spectral MsFEM and RB to achieve low dimensional spaces to compute basis functions at the online stage. In particular, we start with an initial multiscale space that is suitable for the whole range of parameter space. These functions are used to setup a local eigenvalue problem that allows constructing local approximations for the solution. Reduced basis techniques are used to construct small dimensional local problems that allow quickly solving the local eigenvalue problem for the online value of the parameter. The greedy procedure is necessary to pick up the appropriate number of representative fields. Taking the product of important eigenfunctions and initial multiscale basis functions, we compute local basis functions. We discuss various choices for initial multiscale basis functions for our parameter-dependent problem. Numerical results are presented. We discuss that the cost of online computations is low and one can inexpensively solve the global problem. We discuss computational cost and compare the proposed approaches with standard RB methods where global problems are solved to generate reduced space. In particular, we discuss that the proposed approaches have lower computational cost compared to standard RB approaches that use global solutions and the proposed approaches can be easily parallelized.

Although the results presented in this paper are encouraging, there is scope for further exploration. As our intent here was to demonstrate that one can efficiently compute local basis functions, we did not derive rigorous error bounds involving both coarse-scale parameters and reduced basis space dimensions. This error analysis will help us to choose a correct number of local eigenvectors and the dimension of the reduced space and balance these errors. We also plan to study high-contrast problems where the magnitude of the permeability varies continuously. These problems will need large-scale simulations. The applications of the proposed methods to naturally fractured reservoirs is a subject of future research. In particular, we will study how to incorporate known fracture models in local computations and the construction of basis functions (cf. [22]). The extension of the proposed concepts to mass conservative discretization schemes can be helpful in solving coupled flow and transport problems. We would also like to study the design and analysis for initial multiscale spaces and the use of reduced basis concepts in the design of inexact local solves in two-level Schwarz preconditioners.

6 Acknowledgements

YE would like to acknowledge partial support from NSF and DOE. JG would like to acknowledge partial support from DOE. FT would like to acknowledge support from EOARD under Grant FA8655-10-C-4002. We are grateful to anonymous reviewers for their comments that helped to improve the paper.

References

[1] J. E. Aarnes, *On the use of a mixed multiscale finite element method for greater flexibility and increased speed or improved accuracy in reservoir simulation*, SIAM J. Multiscale Modeling and Simulation, 2 (2004), 421-439.

[2] J.E. Aarnes and Y. Efendiev, *Mixed multiscale finite element for stochastic porous media flows*, SIAM Sci. Comp., Volume 30, Issue 5, pp. 2319-2339, 2008. DOI: 10.1137/07070108X.

[3] J. Aarnes and T. Hou, *Multiscale domain decomposition methods for elliptic problems with high aspect ratios*, Acta Math. Appl. Sin. Engl. Ser., 18(1):63-76, 2002.

[4] G. Allaire and R. Brizzi, *A multiscale finite element method for numerical homogenization*, SIAM J. Multiscale Modeling and Simulation, 4(3), 2005, 790-812.

[5] T. Arbogast, G. Pencheva, M. F. Wheeler, and I. Yotov, *A multiscale mortar mixed finite element method*, SIAM J. Multiscale Modeling and Simulation, 6(1), 2007, 319-346.

[6] M. Barrault, Y. Maday, N.C. Nguyen, and A.T. Patera, *An 'Empirical Interpolation' Method: Application to Efficient Reduced-Basis Discretization of Partial Differential Equations*. CR Acad Sci Paris Series I 339:667-672, 2004.

[7] S. Boyoval, *Reduced-basis approach for homogenization beyond periodic setting*, SIAM MMS, 7(1), 466-494, 2008.

[8] S. Boyaval, C. LeBris, T. Lelièvre, Y. Maday, N. Nguyen, and A. Patera, *Reduced Basis Techniques for Stochastic Problems*, Archives of Computational Methods in Engineering, 17:435-454, 2010.

[9] A. Brandt, *Multiscale solvers and systematic upscaling in computational physics*, Computer Physics Communication, 169 (2005) 438-441.

[10] Y. Chen and L. Durlofsky, *Ensemble-level upscaling for efficient estimation of fine-scale production statistics*, SPE Journal, 13, 400-411, 2008.

[11] Z. Chen and T.Y. Hou, *A mixed multiscale finite element method for elliptic problems with oscillating coefficients*, Math. Comp., 72 (2002), 541-576.

[12] L.J. Durlofsky, *Numerical calculation of equivalent grid block permeability tensors for heterogeneous porous media,* Water Resour. Res., 27 (1991), 699-708.

[13] Y. Efendiev and J. Galvis, *A domain decomposition preconditioner for multiscale high-contrast problems*, in Domain Decomposition Methods in Science and Engineering XIX, Huang, Y.; Kornhuber, R.; Widlund, O.; Xu, J. (Eds.), Volume 78 of Lecture Notes in Computational Science and Engineering, Springer-Verlag, 2011, Part 2, 189-196.

[14] Y. Efendiev, J. Galvis and P. Vassielvski, *Spectral element agglomerate algebraic multigrid methods for elliptic problems with high-Contrast coefficients*, in Domain Decomposition Methods in Science and Engineering XIX, Huang, Y.; Kornhuber, R.; Widlund, O.; Xu, J. (Eds.), Volume 78 of Lecture Notes in Computational Science and Engineering, Springer-Verlag, 2011, Part 3, 407-414.

[15] Y. Efendiev, J. Galvis, R. Lazarov, and J. Willems, *Robust domain decomposition preconditioners for abstract symmetric positive definite bilinear forms*, submitted.

[16] Y. Efendiev, J. Galvis, and X. H. Wu, *Multiscale finite element methods for high-contrast problems using local spectral basis functions*, Journal of Computational Physics. Volume 230, Issue 4, 20 February 2011, Pages 937-955.

[17] Y. Efendiev and T. Hou, *Multiscale finite element methods. Theory and applications*, Springer, 2009.

[18] Y. Efendiev, T. Y. Hou, and X. H. Wu, *Convergence of a nonconforming multiscale finite element method*, SIAM J. Num. Anal., 37 (2000), 888-910.

[19] J. Galvis and Y. Efendiev, *Domain decomposition preconditioners for multiscale flows in high contrast media*, SIAM J. Multiscale Modeling and Simulation, Volume 8, Issue 4, 1461-1483 (2010).

[20] J. Galvis and Y. Efendiev, *Domain decomposition preconditioners for multiscale flows in high-contrast media: Reduced dimension coarse spaces*, SIAM J. Multiscale Modeling and Simulation, Volume 8, Issue 5, 1621-1644 (2010).

[21] I. G. Graham, P. O. Lechner, and R. Scheichl, *Domain decomposition for multiscale PDEs*, Numer. Math., 106(4):589-626, 2007.

[22] H. Hajibeygi, D. Karvounis, and P. Jenny, *A hierarchical fracture model for the iterative multiscale finite volume method*, Journal of Computational Physics, 230 (2011) 8729-8743.

[23] T.Y. Hou and X.H. Wu, *A multiscale finite element method for elliptic problems in composite materials and porous media*, Journal of Computational Physics, 134 (1997), 169-189.

[24] T. Hughes, G. Feijoo, L. Mazzei, and J. Quincy, *The variational multiscale method - a paradigm for computational mechanics*, Comput. Methods Appl. Mech. Engrg, 166 (1998), 3-24.

[25] P. Jenny, S.H. Lee, and H. Tchelepi, *Multi-scale finite volume method for elliptic problems in subsurface flow simulation*, J. Comput. Phys., 187 (2003), 47-67.

[26] I. Lunati and P. Jenny, *Multi-scale finite-volume method for compressible multi-phase flow in porous media*, J. Comp. Phys., 216:616-636, 2006.

[27] L. Machiels, Y. Maday, I.B. Oliveira, A.T. Patera, and D.V. Rovas, *Output bounds for reduced-basis approximations of symmetric positive definite eigenvalue problems*, Comptes Rendus de l'Académie des Sciences, 331(2):153-158, 2000.

[28] Y. Maday, *Reduced-basis method for the rapid and reliable solution of partial differential equations*. In: Proceedings of international conference of mathematicians, Madrid. European Mathematical Society, Zurich, 2006.

[29] T. P. A. Mathew, *Domain decomposition methods for the numerical solution of partial differential equations*, volume 61 of *Lecture Notes in Computational Science and Engineering*, Springer-Verlag, Berlin, 2008.

[30] N. C. Nguyen, *A multiscale reduced-basis method for parameterized elliptic partial differential equations with multiple scales*, J. Comp. Physics, 227(23), 9807-9822, 2008.

[31] H. Owhadi and L. Zhang, *Metric based up-scaling*, Comm. Pure and Applied Math., vol. LX:675-723, 2007.

[32] H. Owhadi and L. Zhang, *Localized bases for finite dimensional homogenization approximations with non-separated scales and high-contrast*, submitted to SIAM MMS, Available at Caltech ACM Tech Report No 2010-04. arXiv:1011.0986.

[33] G. Rozza, D. B. P Huynh, and A. T. Patera, *Reduced basis approximation and a posteriori error estimation for affinely parametrized elliptic coercive partial differential equations. Application to transport and continuum mechanics*. Arch Comput Methods Eng 15(3):229?275, 2008.

[34] M. Sarkis, *Nonstandard coarse spaces and Schwarz methods for elliptic problems with discontinuous coefficients using non-conforming elements*, Numer. Math., 77(3), 383-406, 1997.

[35] A. Toselli and O. Widlund. *Domain decomposition methods—algorithms and theory*, volume 34 of Springer Series in Computational Mathematics, Springer-Verlag, Berlin, 2005.

[36] X.H. Wu, Y. Efendiev, and T.Y. Hou, *Analysis of upscaling absolute permeability*, Discrete and Continuous Dynamical Systems, Series B, 2 (2002), 185-204.

[37] J. Xu and L. Zikatanov, *On an energy minimizing basis for algebraic multigrid methods*, Comput. Visual Sci., 7:121-127, 2004.

[38] H. Zhou and H.A. Tchelepi, *Two-Stage Algebraic Multiscale Linear Solver for Highly Heterogeneous Reservoir Models*, SPE J. SPE-141473-PA.